Magri, F., Cacace, M., Fischer, T., Kolditz, O., Wang, W., Watanabe, N. (2017): Thermal convection of viscous fluids in a faulted system: 3D benchmark for numerical codes. - *Energy Procedia*, *125*, pp. 310—317.

DOI: http://doi.org/10.1016/j.egypro.2017.08.204

Available online at www.sciencedirect.com

ScienceDirect

Energy Procedia 125 (2017) 310–317

Energy Procedia

www.elsevier.com/locate/procedia

European Geosciences Union General Assembly 2017, EGU Division Energy, Resources & Environment, ERE

Thermal convection of viscous fluids in a faulted system: 3D benchmark for numerical codes

Fabien Magri[a,b,*], Mauro Cacace[c], Thomas Fischer[a], Olaf Kolditz[a], Wenqing Wang[a], and Norihiro Watanabe[a]

[a]*Helmholtz Centre for Environmental Research – UFZ, ENVINF, Leipzig,Germany*
[b]*Freie Universität Berlin, Hydrogeology, Berlin, Germany*
[c]*GFZ German Research Centre for Geosciences, Section 6.1 - Basin Modelling, Potsdam, Germany*

Abstract

We propose a new benchmark for the simulation of thermal convection in a 3D faulted system. Linear stability analysis is adopted to estimate the critical viscous-dependent Rayleigh number. These results are used to quantify the reliability of OpenGeoSys-5, Golem and FEFLOW simulators in accounting for the onset conditions and in predicting the long-term behavior of convective flow patterns. By comparing the analytical and numerical results, we can conclude that the proposed methodology and Rayleigh expressions can be applied as benchmark case for any numerical study involving coupled hydrothermal fluid flow in fault zones.

Peer-review under responsibility of the scientific committee of the European Geosciences Union (EGU) General Assembly 2017 – Division Energy, Resources and the Environment (ERE).

Keywords: Fault; Convection; Rayleigh; Simulation; OpenGeoSys; Moose

1. Introduction

Free thermal convection of viscous fluid in porous media is a process relevant for a wide variety of problems related to practical aspects of engineering processes. Examples of these applications include, but are not limited to:

* Corresponding author. Tel.: +49-341-235-1098; fax: +49-341-235-1939.
E-mail address: fabien.magri@ufz.de

1876-6102
Peer-review under responsibility of the scientific committee of the European Geosciences Union (EGU) General Assembly 2017 – Division Energy, Resources and the Environment (ERE).
10.1016/j.egypro.2017.08.204

(1) fresh-salt water intrusion in coastal regions; (2) upconing of brackish water and their mixing with surface fresh water lenses; (3) flow instabilities around salt domes and their effects on the cap rock behavior of these geological barriers for geological storage; and (4) geothermal heat production near the well bore areas and along pre-existing fault zones. The main characteristic of convective flows is that they are influenced by, even small, fluid density and viscosity gradients giving rise to self-sustained (aka self-perturbing) and highly non-linear flow dynamics.

In this paper, we focus in quantifying, via analytical and numerical approaches, onset conditions and first order characteristics of the long-term behavior of convective flow instabilities across major fault zones. Despite the ubiquitous presence of faults in the subsurface and their relevance for geo-engineering applications, the dynamics of convective flows in fault zones is still relatively unexplored. Exceptions are the works from [1-3].

Indeed no analytical solution of the strongly coupled partial differential equations (PDEs) of the convective problem exists. Therefore, it is not known whether the development of the perturbation as depicted in coupled hydrothermal simulations might reflect the actual, i.e. physical instability of the fluid or whether it is caused by instability of the numerical, therefore unphysical, integration of the governing equations.

Here, an attempt to rule out unphysical disturbances on convective related studies is described. We provide an analytical solution to the problem, which we propose as a benchmark case to quantify the reliability and robustness of numerical analysis of these types of problems and test the validity of our approach by solving the proposed benchmark with three finite element software, OpenGeoSys-version5 (OGS) [4], Golem [5] and FEFLOW [6].

Nomenclature

Ra	Rayleigh number [1]
Ra_{Crit}	Critical Rayleigh number
k	Hydraulic permeability [m^2]
ρ_0	Fluid density at $T=T_c$ [kg/m^3]. In this example, ρ_0=1022.38 kg/m3
c_f	Specific fluid heat capacity [J/kg/°C]
g	Gravity [m^2/s]
β	Fluid thermal expansion [1/°C] to fit fluid density Eq.5 In this example, β=5.9e-4 $°C^{-1}$
T_h	Bottom boundary condition (hot) [°C]. In this example, T_h=170°C
T_c	Top boundary condition (cold) [°C]. In this example, T_c=20°C
T_v	Approximation temperature [°C] to fit fluid viscosity Eq.5. In this example, T_v=62.1°C
T_{init}	Initial temperature
H	Fault height [m]. In this example, H=5500m
ϕ	Fault porosity [1]
$\lambda_{f,s}$	Fluid, solid heat conductivity [J/ m/s/°C]
λ_b	Bulk heat conductivity [J/ m/s/°C]; $\lambda_b=\phi\lambda_f+(1-\phi)\lambda_s$
μ_0	Fluid viscosity at $T=T_c$ [Pa/s]. In this example, μ_0=1.17e-3 Pa/s
2δ	Fault width [m]. In this example, 2δ=40m
Δ	Half of aspect ratio [1], $\Delta=\delta/H$. In this example, Δ=3.64e–3
γ	Dimensionless temperature [1], $\gamma=T_h-T_c/T_v$ Eq. 4. In this example, γ=170-20/62.1=2.42

2. Methods and results

2.1. Problem description and linear stability analysis

Figure 1a illustrates the setup of the model used in this study, as adapted from [7]. The geometry of the model domain consists of a 40 m wide (2δ), 5500 m long (H) fault (half aspect ratio $\Delta = \delta/H$ = 3.64e-3) surrounded by an impervious rock matrix (5500x5500x5500 m in lateral and vertical dimensions). The matrix-fault system is isothermally heated from below by an imposed constant temperature along the basal boundary (T_h=170°C). The temperature at the top surface is also kept constant and equal to T_c=20°C, thus resulting in an overall thermal gradient of 27.3°C/km.

All boundaries are closed to fluid flow. Fluid density and viscosity are considered a function of temperature, while all other parameters are considered constant according to Table 1.

Table 1. Physical properties of fluid, fault and enclosing rocks. Fluid EOS are given in Fig. 1b

Property	Fluid	Fault	Enclosing Rocks
k [m^2]	-	1.019e-13	1e-18
$\lambda_{f,s}$ [J/ m/s/°C]	0.65	2	2
$\rho_{f,s}c_{f,s}$ [J/m^3/°C]	4.2e6	2.5e6	2.5e6
ϕ [1]	-	0.5	1e-3

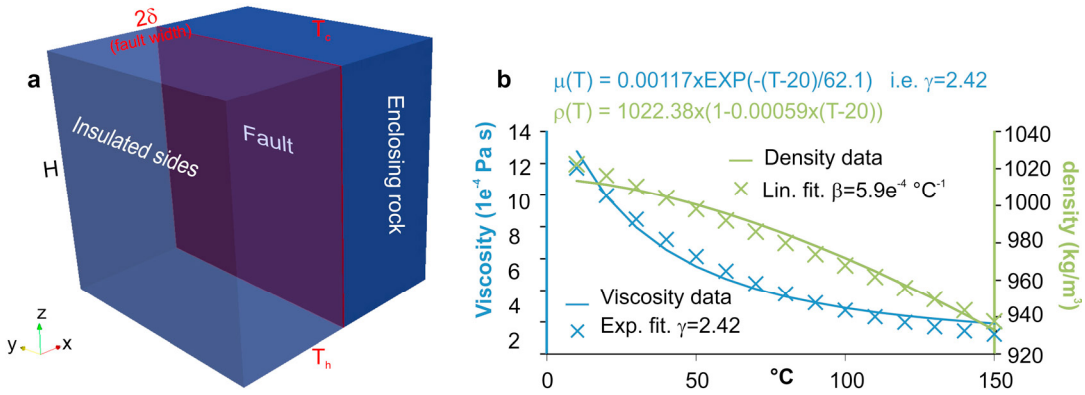

Fig. 1. (a) 3D faulted block heated from below; (b) Temperature-dependent fluid density and viscosity in the range T_h=170 °C and T_c=20 °C

The equations of state (EOS) considered in the present study are based on [1] and consider a linear dependency of fluid density on temperature and an exponential dependency of fluid viscosity on temperature (Fig. 1b), as:

$$\mu(T) = \mu_0 \cdot \exp\left(-\frac{T-T_c}{T_v}\right) \;\; ; \;\; \rho(T) = \rho_0 \cdot \left(1-\beta(T-T_c)\right) \tag{1}$$

In the 3D section, we present also the results obtained by numerical simulations considering a more realistic EOS for both fluid density and viscosity as based on the latest IAPWS release [8].

The system is initially destabilized by adding a thermal perturbation within the fault plane, the latter considered as an equivalent porous medium (EPM), in the form of $\varepsilon(x,y,z,t=0)=\sin(\pi z)\cos(\pi y)$. This instability will trigger convective flow pattern within the fault plane, the onset conditions of which is the subject of the study. According to classical linear instability analysis, under infinitesimal perturbation the Rayleigh number of the fault domain at constant fluid viscosity (top temperature condition, T_c) reads as:

$$Ra = \frac{k\rho_0^2 c_f g\beta\left(T_h - T_c\right)H}{\lambda_b\,\mu_0} \tag{2}$$

whith $\mu_0=\mu(T_c)$.

Thermal convection in a faulted system saturated with a liquid-phase fluid occurs when [7]:

$$Ra > Ra^{crit}(\Delta,\gamma) = \left[\left(\frac{8.19}{\Delta}\right)^{5/4} + \left(4\pi^2\right)^{5/4}\right]^{4/5} \left(1+0.493\gamma+0.12\gamma^2\right)e^{-\gamma} \quad (3)$$

With

$$\Delta = \frac{\delta}{H} \quad (4)$$

is half of the fault aspect ratio, and

$$\gamma = \frac{T_h - T_c}{T_v} \quad (5)$$

is a dimensionless temperature that characterizes the viscous property of the saturating fluid (Fig. 1b).

Given the parameters listed in Table 1, the Rayleigh number of the fault is Ra≈1348.5 (Eq. 1). Under the thermal gradient considered in the present study, the optimal fit for the fluid viscosity has been obtained with $\gamma = 2.42$. By replacing this value into the RHS of Eq. 3, we can predict the onset of thermal convection for a fault having a 4 times lower permeability than for a fault saturated with fluid of constant viscosity (γ=0). Indeed, at Δ=3.64e−3 and γ=2.42 , according to Eq. 3, the onset of convection is triggered at critical Rayleigh number $Ra_{crit}(\gamma=2.42)\approx 587$. On the other hand, if we fix fault permeability, a system saturated with temperature-dependent viscous fluid will convect under a thermal gradient 4 times lower than if the fluid viscosity was constant.

In the next paragraph, we will make use of numerical investigations to further quantify onset conditions and temporal behavior of predicted convective instabilities.

2.2. Modelling results – 2D case

Before discussing the 3D scenario, simulations were carried out for a 2D case, that is, a case that considers only the fault pane. This was done in order to test the reliability of the different simulators used, at the same time offering a gentle introduction to the modeling. A perfect match among the results from the three simulators is evident both with respect to the evolution of the linear perturbation as well as for the thermal anomaly (Fig. 2).

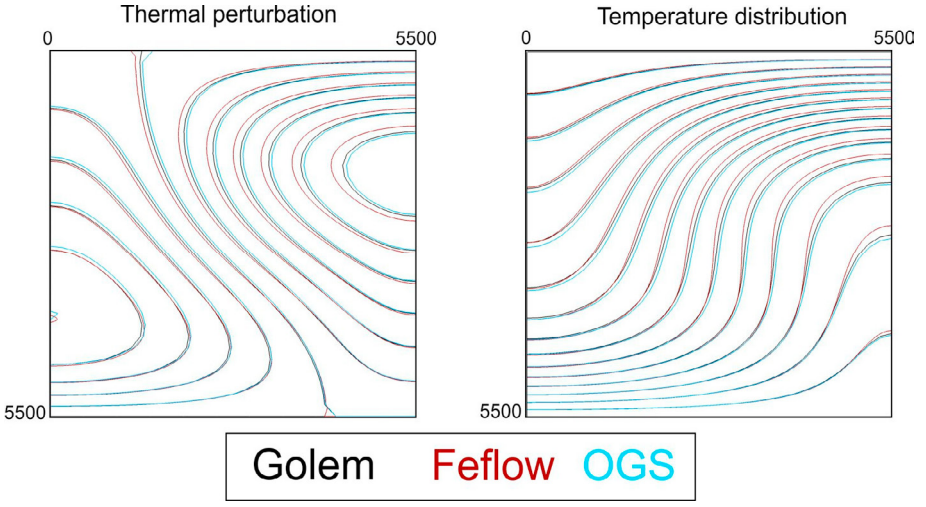

Fig. 2. Contours of the perturbation (left) and of the temperature (right) as obtained at the end of the simulation (end time 1e+13 s) by the three simulators, 2D case.

In agreement with the theory, under such conditions a convective cell evolves in the right part of the model domain as also visible by inspecting the fluid velocity plot in Figure 3.

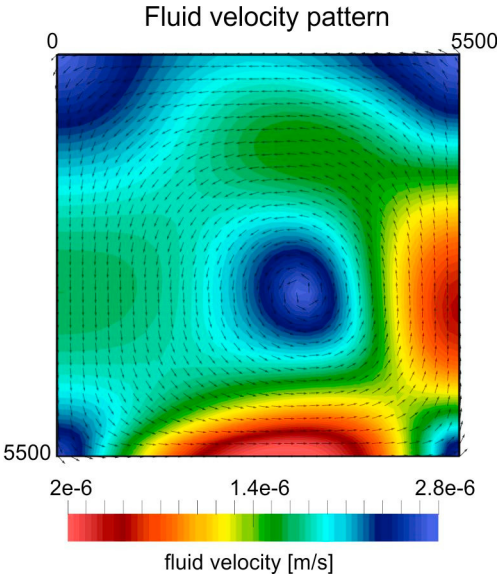

Fig. 3. Fluid velocity (m/s) calculated with Golem displaying one convective cell in the fault plane (temperature dependent viscosity and density). The results from the other simulators show similar characteristics.

For simulations in which isoviscous conditions are considered, no convective instability evolves (Fig. 4), and fluid velocity are up to six orders of magnitude lower than for the viscous case, as expected from the theory.

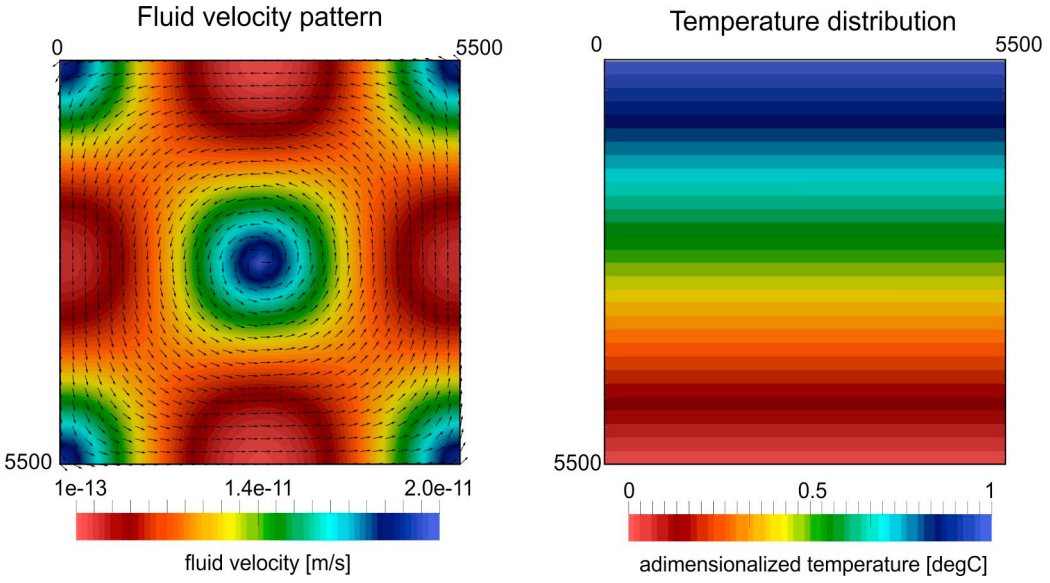

Fig. 4. Fluid velocity (m/s) and temperature profile at constant viscosity condition calculated with Golem. In agreement with the theory, due to the parameter setting, the system is below the critical value for convective flow and no convective thermal disturbances develop. Results from the other simulators show similar characteristics.

2.3. Modelling results – 3D case

In this second part, we investigate the reliability of the three simulators to capture onset conditions and long-term characteristics of convective instabilities for a 3D case. The parameters are the same as adopted for the 2D case, and are summarized in Table 1. Based on the parameterization, the theory predicts convective instabilities and unstable conditions. Indeed, all simulators display onset of thermal convection in the fault plane (Fig. 5). Qualitatively the patterns are similar. However, differences can be observed in the details of the convective flow patterns, with the results from the three simulators all display a different number of convective cells (e.g. 4 cells in FEFLOW, 3 cells in OGS and Golem) and temperature maxima.

Here it is worth recalling that in density-driven flow problems different spatial and temporal discretization can induce numerical instabilities which propagation will modify developing fingers. While the input mesh has been kept the same, the time discretization adopted by the three different solvers varies. In an attempt to minimize this source of potential errors, we have imposed the same conditions to the maximum time step size, here fixed at 1e+10 s, so not to violate the Courant criterion. Therefore the different temporal evolution of the initial temperature perturbation can be attributed to an uncontrolled propagation of instabilities due to the type of solver and error tolerances as well as different type of numerical implementations (e.g. weak coupling in OGS and FEFLOW vs. monolithic in Golem).

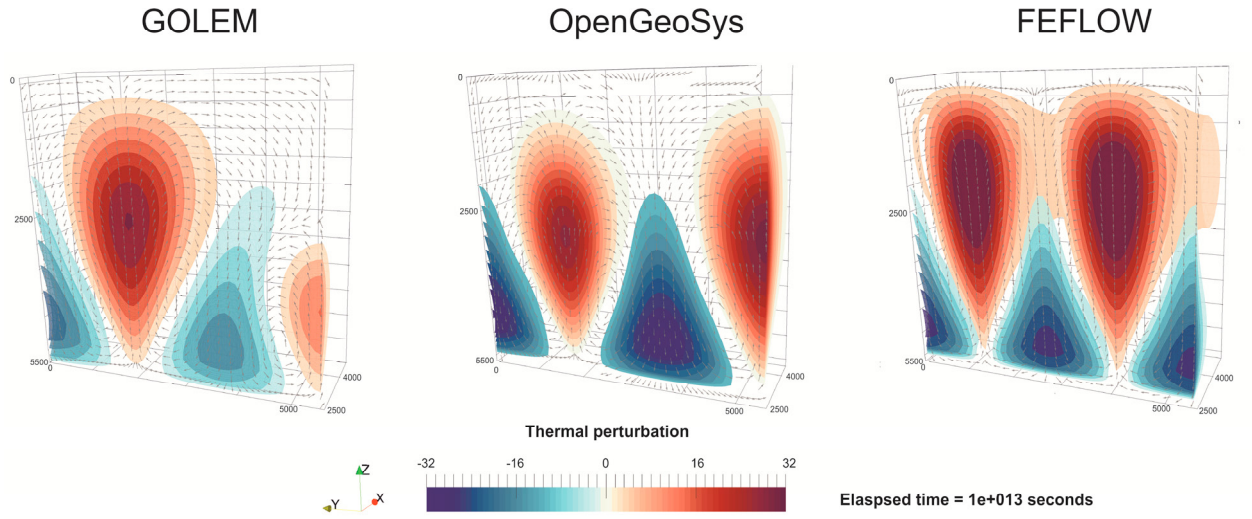

Fig. 5. Calculated temperature perturbation (T-T_{init}) °C at t=1e13 s along the fault plane (Golem, OGS and FEFLOW).

An additional scenario that takes into account the IAPWS [8] formulation of fluid density and viscosity is run with OGS [4] and Golem [5] (Fig. 6). It was not possible to run this scenario with FEFLOW [6], due to current limitations in the API functionalities of the software. Results obtained with the IAPWS formulation [8] indicate the onset of a more intense convective flow with respect to the simplified EOS (compare Fig. 6 and Fig. 5): For example, Golem simulations display an additional convective cell and OGS perturbation patterns cover wider areas of the fault plane.

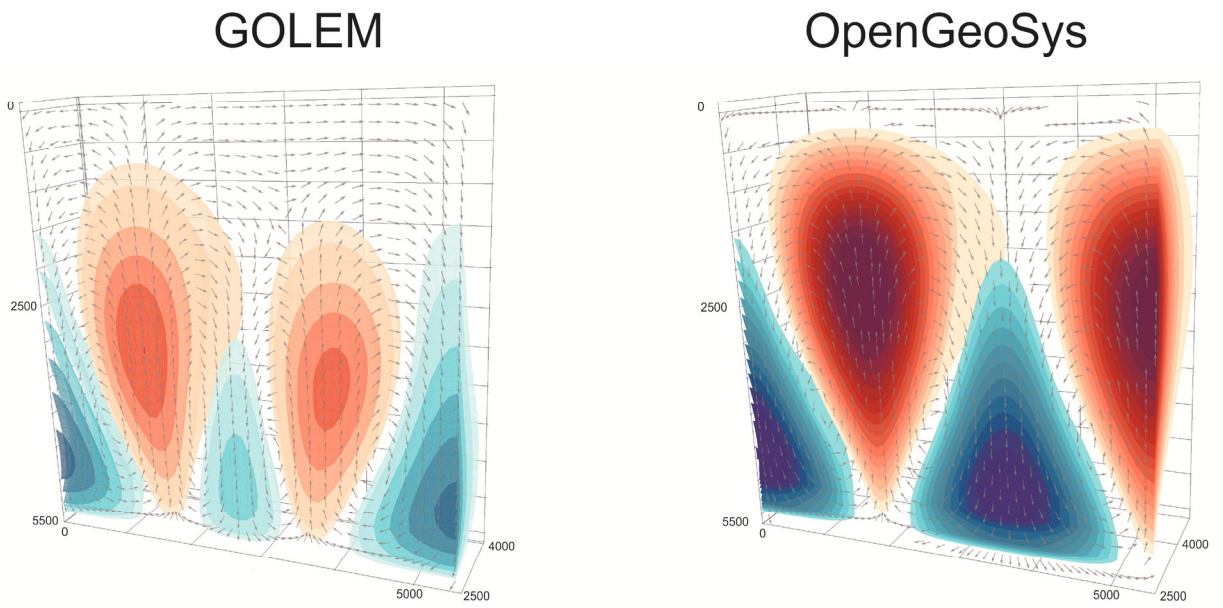

Fig. 6. Calculated temperature perturbation ($T-T_{init}$) °C at t=1e13 s along the fault plane (Golem, OGS) using the IAPWS formulation [8]

4. Summary

A numerical benchmark for the simulations of thermal convection onset of a single-phase fluid with temperature dependent viscosity in a vertical permeable fault is proposed. Three different finite elements, OGS [4], Golem [5], and FEFLOW [6], successfully simulated the onset of thermal convection at critical Rayleigh numbers inferred from the linear stability analysis [7]. Owing to the strong coupling of the PDE, the numerical solutions are highly sensitive to discretization errors (spatial/temporal) and solver settings as well as to the used EOS. Consequently, the calculated patterns are all qualitatively similar while differences in the calculated values exist. Results of case-studies (e.g. basin systems) must be interpreted carefully and require additional constraints (field data).

The given example provides a useful benchmark that can be applied to any numerical code of thermally-driven flow processes at basin-scale.

Acknowledgements

We greatly acknowledge the DFG (grant Ma4450/2-3) for the financial support.

References

[1] Wang, M., Kassoy and D.R.,Weidman, P.D. (1987) „Onset of convection in a vertical slab of saturated porous media between two impermeable conducting blocks.” *Int. J. Heat Mass Transf.* 30 (1987):1331-1341.

[2] Zhao, C., Hobbs, B.E. and Ord, A. (2008) “Convective Heat Transfer within Three dimensional Vertical Faults Heated from below”, in *Convective and Advective Heat Transfer in Geological Systems,* Springer, Berlin Heidelberg

[3] Tournier, C., Genthon, P., and Rabinowicz, M. (2000) „The onset of natural convection in vertical fault planes: consequences for the thermal regime in crystalline basements and for heat recovery experiments.” *Geophys. J. Int.* 140 (2000): 500-508.

[4] Kolditz, O., Bauer, S., Bilke, L., Böttcher, N., Delfs, J. O., Fischer, T., U. J. Görke, T. Kalbacher, G. Kosakowski, McDermott, C. I., Park, C. H., Radu, F., Rink, K., Shao, H., Shao, H.B., Sun, F., Sun, Y., Sun, A., Singh, K., Taron, J., Walther, M., Wang,W., Watanabe, N., Wu, Y., Xie, M., Xu, W. and Zehner, B. (2012) „OpenGeoSys: an open-source initiative for numerical simulation of thermo-hydro-mechanical/chemical (THM/C) processes in porous media“, *Environmental Earth Sciences.* 67(2) (2012): 589-599.

[5] Cacace, M. and Jacquey, A.B. (2017): Flexible parallel implicit modelling of coupled Thermal-Hydraulic-mechanical processes in fractured rocks. *Solid Earth Discuss*., doi:10.5194/se-2017-33.

[6] Diersch, H.-J.G. (2014) “FEFLOW: Finite Element Modeling of Flow, Mass and Heat Transport in Porous and Fractured Media.” Springer, Verlag Berlin Heidelberg

[7] Malkovsky, V. I. and Magri, F. (2016) “Thermal convection of temperature-dependent viscous fluids within three-dimensional faulted geothermal systems: estimation from linear and numerical analyses” *Water Resour. Res.,* 52 (2006): 2855–2867.

[8] IAPWS Industrial Formulation 1997 for the Thermodynamic Properties of Water and Steam (2008) “International Steam Tables: Properties of Water and Steam Based on the Industrial Formulation IAPWS-IF97.” Springer Berlin Heidelberg, Berlin, Heidelberg